Water retention curve of clayey sands determined from pore structure by using various methods

Quoc-Hung Vu, *Jean-Michel* Pereira, and *Anh Minh* Tang

Navier, Ecole des Ponts, Univ Gustave Eiffel, CNRS, Marne-la-Vallée, France

Abstract. Besides standard approaches, the soil water retention curve (SWRC) can be estimated either from pore size distribution obtained by mercury intrusion porosimetry or from the soil freezing characteristic curve. These methods are based on simplified laws such as Young-Laplace for capillary suction or Clausius-Clapeyron for cryo-suction. These laws might not be valid for clayey sands where the presence of clay particles would induce other water retention mechanisms. This study aims to assess the clay content's effect on the validity of these two methods in determining the SWRC of clayey sands. Clay sands were prepared at different clay contents by mixing pure sand with kaolin clay prior to compaction at the Proctor maximum dry density. Five clay contents (dry mass of clay divided by dry mass of soil) were considered (0, 5, 10, 15, and 20%). The reference SWRC was obtained by standard suction measurements. The results show that SWRCs estimated from mercury intrusion porosimetry and soil freezing characteristic curve are generally in agreement with the reference SWRC. However, the results obtained by the soil freezing characteristic curve are limited in terms of suction range (500 to 5 MPa) which is not appropriate for clayey sands, while those from mercury intrusion porosimetry show significant discrepancy because of the structure heterogeneity obtained by Proctor compaction.

1 Introduction

The soil water retention curve (SWRC) describes the relationship between water content and suction. This curve plays an important role in modelling the coupled hydro-mechanical behaviour of unsaturated soils [1–3]. SWRC is conventionally determined from suction measurement [4, 5] or control [6, 7] following drying and/or wetting processes.

Soil suction (s) generally includes two components (matric and osmotic) and matric suction is generally the most dominant component in sandy soils in the case without salt presence. By using the Young-Laplace equation [8, 9], matric suction in porous media can be estimated from pore radius. For this reason, SWRC can also be estimated from the pore size distribution (PSD), which is usually determined by mercury intrusion porosimetry (MIP) [10, 11], by using Laplace's equation [12, 13]. However, SWRC obtained from MIP and SWRC obtained by conventional methods generally do not agree for fine-grained soils [14] probably due to pore trapping effect or water and dissolved salts effect on clay fabric compared to the process of mercury intrusion[15].

Besides, soil matric suction can be determined from freezing temperature by using Clausius-Clapeyron equation [16]. However, the consistency between SWRC obtained from soil freezing characteristic curve and that obtained by conventional methods remains questionable because of the complexity of the mechanisms associated with freezing-thawing compared to drying-wetting, such as supercooling, different contact angles [17], accuracy of water content measurement [18] and assumptions behind Clausius-Clapeyron equation [19, 20].

Among factors such as dry density, grain nature, grain size distribution, etc., fines content influences significantly SWRC [21, 22]. Several studies investigated SWRC of sandy soils with different clay contents [23–26] and found that the SWRC of soil with higher clay content has a lower steepness, a higher air entry suction and a higher residual suction. In addition to the aforementioned effects, increasing clay content from 30% to 100% by dry weight may enlarge the hysteresis of SWRC [27]. For soils with low clay content (0% to 8%), SWRC shows a clear bimodal shape, which is strongly dependent on fines content [28].

This study aims at assessing the effect of clay content on the validity of using mercury intrusion porosimetry and soil freezing characteristic curve in determining SWRC of clayey sands. Clayey sands were prepared at different clay contents by mixing pure sand with kaolin clay prior to the compaction at the Proctor maximum dry density. Five clay contents (dry mass of clay divided by dry mass of soil) were considered (0, 5, 10, 15, and 20%). The reference SWRC was obtained by standard suction measurements. SWRC obtained by the three methods were compared. The results were finally analysed to identify the main mechanisms explaining the effect of fines content on the soil water retention curve.

2 Material and experimental methods

Table 1. Physical properties of Fontainebleau sand.

Property	Value
Median grain size, $\boldsymbol{D_{50}}$(mm)	0.21
Uniformity coefficient, $\boldsymbol{C_U}$	1.52
Minimum void ratio, $\boldsymbol{e_{min}}$	0.54
Maximum void ratio, $\boldsymbol{e_{max}}$	0.94
Particle density, $\boldsymbol{\rho_s}$ (Mg/m^3)	2.65
Minimum dry density, $\boldsymbol{\rho_{d,min}}$ (Mg/m^3)	1.37
Maximum dry density, $\boldsymbol{\rho_{d,max}}$ (Mg/m^3)	1.72

Fontainebleau sand and Speswhite Kaolin clay (whose physical properties are shown in Table 1 and Table 2, respectively) were mixed at various clay contents in dry mass (see Table 3 and Fig. 1). Each mixture was wetted at optimal water content [29] and packed in a plastic bag for at least 24 h for moisture distribution homogenization prior to compaction in a rigid metallic cylindrical mould (150 mm in height and 150 mm in diameter).

Table 2. Physical properties of Speswhite Kaolin clay.

Property	Value
Liquid limit, LL (%)	55
Plastic limit, PL (%)	30
Plasticity index, PI	25
Specific surface area (m^2/g)	0.94
Particle density, ρ_s (Mg/m^3)	2.65
Particle diameter < 0.002 mm (%)	79
Particle diameter > 0.01 mm (%)	0.5
Maximum dry density, $\rho_{d,max}$ (Mg/m^3)	1.45

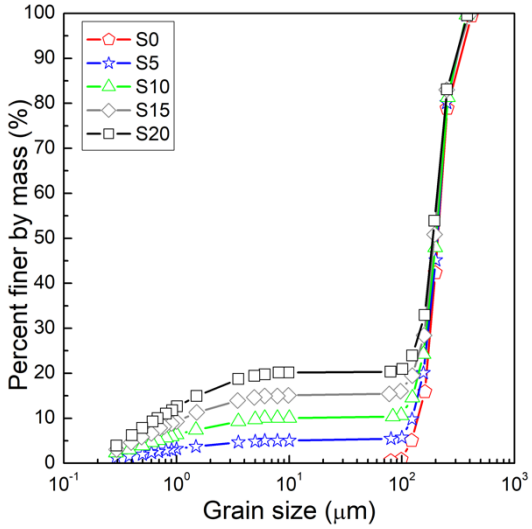

Fig. 1. Grain size distribution curves of tested soils.

Table 3. Physical properties of samples.

Soil	Clay content (%)	Water content w (%)	Dry density ρ_d (Mg/m^3)	Porosity n (-)
S0	0	0.21	1.70	0.36
S5	5	0.19	1.77	0.33
S10	10	0.14	1.93	0.27
S15	15	0.13	1.99	0.25
S20	20	0.13	1.96	0.26

To determine the reference SWRC following the suction measurement method [30], after soil compaction in a mould, three sensors were carefully inserted inside the sample (Fig. 2 and Fig. 3): (i) a tensiometer T8 (1 kPa in accuracy) to measure matric suction (s) [4]; (ii) a time domain reflectometry probe ThetaProbe ML2x (1% in accuracy) to measure volumetric water content (θ_w); (iii) and a KD2-Pro probe to measure the soil thermal conductivity (whose data were not analysed in this study). Afterwards, the sample was saturated by injecting water from its bottom (during 0.5 to 2 days depending on fines content) until a layer of water of 10 mm was visible on the top of the specimen. To dry the specimen, two holes created on the top cover were opened to allow evaporation from the top surface (Fig. 3). After a certain duration, the two holes were covered by two lids to prevent moisture exchange with the atmosphere. The equilibrium was reached after several hours prior to the next step; this procedure is similar to that used by Nguyen et al. [31]. Once suction excesses the capacity of the tensiometer (100 kPa), one small piece of soil was extracted from the sample to determine SWRC within a drying-wetting path by using a chilled-mirror dew-point hygrometer (WP4C) following the procedure used by Wang et al. [32].

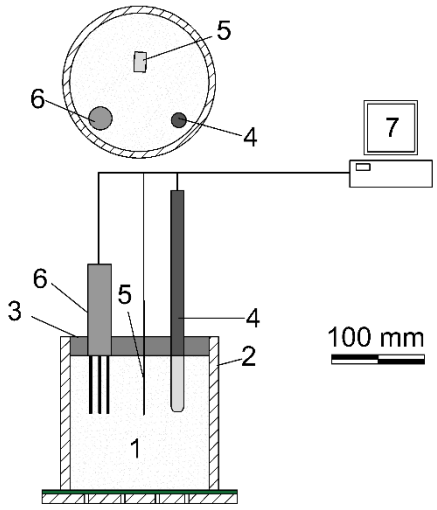

Fig. 2. Schematic view of the experimental device used for suction measurement. (1) Soil; (2) Metallic cylindrical cell; (3) Insulating cover; (4) Tensiometer; (5) Thermal conductivity probe; (6) Soil water content sensor; (7) Data logging system.

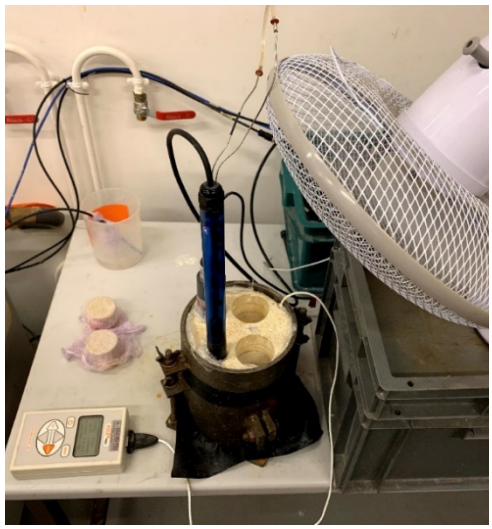

Fig. 3. View from the top of the experimental device used for suction measurement.

For MIP tests, small samples (less than 1 g) were extracted from the compacted specimen using a cutter and freeze-dried by the procedure proposed by Delage and Pellerin [33] prior to conducting mercury intrusion.

For thawing tests, after soil compaction, sensors were installed as shown in Fig. 4. Beside tensiometer and KD2-Pro probe, whose data were not analysed in this study, a ThetaProbe and a temperature sensor (PT100, accuracy ±0.03 °C) were used. Afterwards, soil specimen was saturated prior to being installed in the temperature-controlled bath. To perform the test, soil temperature (T) was first decreased down to -2 °C or -3 °C to

freeze soil water. It was afterwards increased in steps of 0.2 °C until 0 °C to thaw the frozen soil.

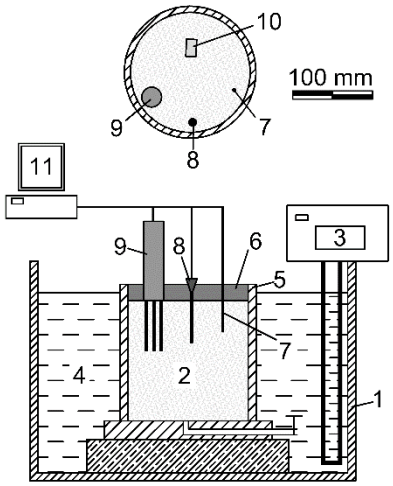

Fig. 4. Schematic view of the experimental setup used for freezing-thawing tests. (1) Temperature-controlled bath; (2) Soil specimen; (3) Temperature controlling system; (4) Temperature-controlled liquid (30% ethylene glycol + 70% water); (5) Metallic cylindrical cell; (6) Insulating cover; (7) Temperature sensor; (8) Tensiometer; (9) Soil water sensor; (10) Thermal conductivity probe; (11) Data logger system.

3 Results

Similar pattern can be observed on SWRC obtained by conventional method (Fig. 5), data for pure sand (S0) was taken from the study of Doussan and Ruy (2009). From saturated state (degree of saturation S_r = 100%), suction increase induced a first decrease of S_r at $s \sim 5$ kPa. Afterward, S_r decreased with a lower rate. When suction exceeded 1000 kPa, S_r decreased again with a higher rate. For suction higher than 5000 kPa, S_r decreased with a smaller rate. At a given suction, S_r was higher for a higher clay content. In addition, for the same soil at the same suction, S_r was slightly smaller during the wetting path than during the drying path. The hysteresis effect of SWRC can be mostly attributed to pore blocking and capillarity. The fact of adding fines in sandy soil changed the arrangement of pores. The latter made clearer hysteresis effect of SWRC in soils with higher fines content. The wetting path was stopped at suction of around 500 kPa because WP4C is less accurate at suction lower than this value. This bimodal shape has been observed by Zhang et al. [28] on well-graded gravel mixed with 0 – 8% of Kaolin clay and explained by the dual porosity (micropores between clay particles and macropores between grains).

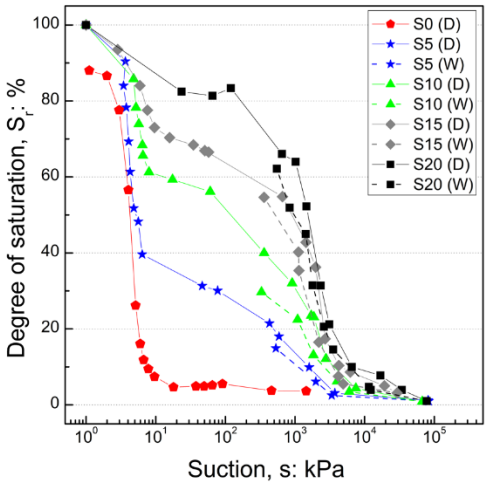

Fig. 5. SWRC obtained by the conventional method.

Actually, results of MIP tests, Fig. 6, show clearly two families of pores: macropores (entrance pore diameter d = 20 – 100 µm) and micropores (d = 0.1 – 1 µm). The volume of macropores was higher at a lower clay content. Note that tests with S10, S15, and S20 were replicated showing a certain discrepancy. In addition, MIP test could not be performed on pure sand (S0). The bimodal SWRC (Fig. 5) can thus be clearly explained by the double porosity observed with MIP test (Fig. 6). The results of this study evidence the effect of fines content on water retention in the high suction range (> 500 kPa) which corresponds to micropores. The discrepancy between MIP results (Fig. 6) can be explained by the material preparation method. Small samples (less than 1 g) were extracted from large specimens mixed and compacted using the Normal Proctor method. In addition, the mixing order (sand-clay-water) and the water content at compaction in the present study could lead to heterogeneous microstructure after Yin et al. [35].

All the results of the thawing path obtained during the freezing/thawing tests (Fig. 7) show an increase of θ_w when T increased, indicating the progressing thawing process. Thawing occurred significantly at temperature close to 0 °C for all soils. At a given temperature, soil with higher clay content had higher θ_w.

Results of MIP and thawing tests were then used to estimate SWRC. For MIP test, Laplace equation that links the capillary pressure to the interfacial properties of the fluids-solid system with entrance pore entrance diameter d was applied to obtain the relationship between matric suction and mercury intrusion pressure u_{Hg} [14]:

$$s = 0.196\, u_{Hg} \quad (1)$$

Water content was calculated from the change of intruded mercury void ratio e_M by assuming that water content is null at the highest suction (40 MPa).

Clausius-Clapeyron equation was used to estimate suction during thawing:

$$s = L_f \rho_w \frac{T - T_f}{T_f} \quad (2)$$

where $\rho_w = 1000$ kg/m^3 is the density of water, $L_f = 334$ kJ/kg is the latent heat of fusion of water, $T_f = 273.15\ K$ is the freezing point of water.

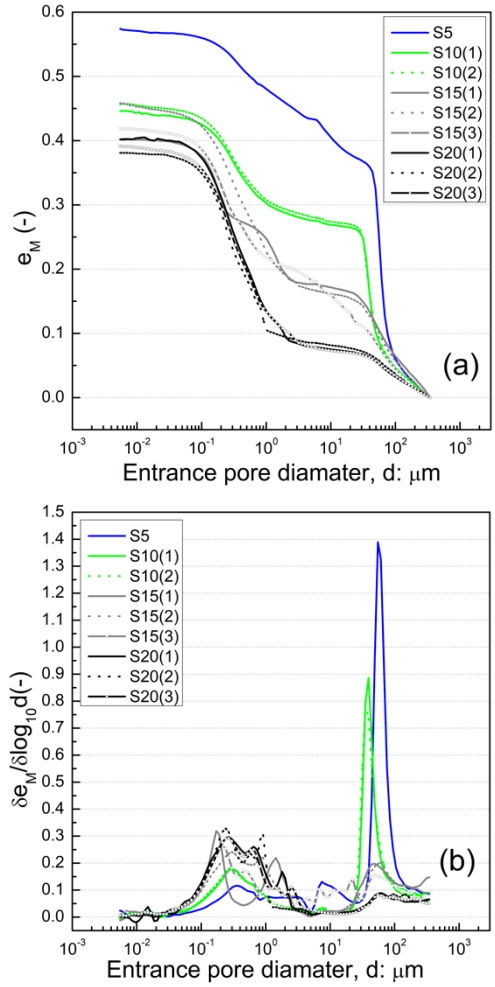

Fig. 6. Results of MIP tests: (a) Intruded mercury void ratio and (b) Pore size density function as a function of the entrance pore diameter.

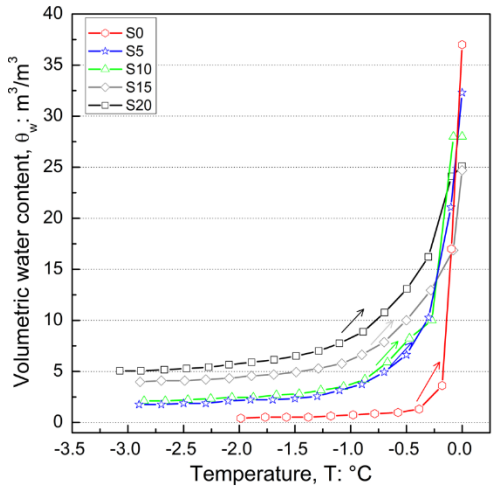

Fig. 7. Results obtained on the thawing path of freezing/thawing tests: volumetric unfrozen water content as a function of the temperature.

Fig. 8 shows SWRCs derived from the three methods for each soil. Generally, the results of MIP should be compared with the drying path while the results of the thawing test should be compared with the wetting path. For clean sand S0, data on the wetting path were not available. Anyway, results obtained by thawing are in good agreement with the drying path (which should be similar to the wetting path for this material in the range of suction available with the thawing method, i.e. 500 kPa – 3 MPa). For S5, results from MIP is in good agreement with the drying path for the whole range of suction while results from the thawing test are in good agreement with the wetting path (both are limited to suctions higher than 500 kPa). For S10 and S20, observations similar to S5 can be made even if the agreement between MIP and drying path is less obvious, which is consistent with the conclusions by [14]. For S15, a notable discrepancy between the MIP results of can be observed. The difference between SWRCs obtained by the various methods remains smaller than this discrepancy.

For all soils, results of MIP tests show generally a smaller water content (compared to the other methods) at suction higher than 1000 kPa. This difference is more notable at higher clay content. This phenomenon can be explained by the role played by water adsorption on clay particles on the water retention properties of the soil, which cannot be predicted by MIP data and its interpretation based on capillary suction effects.

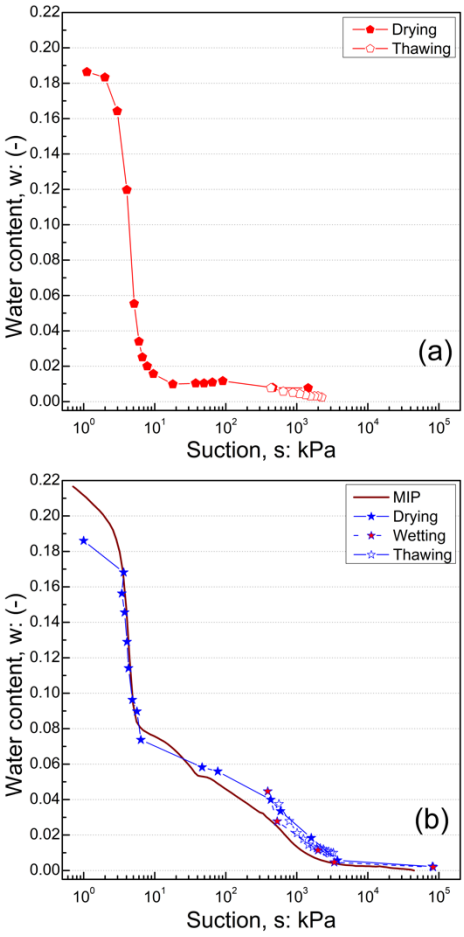

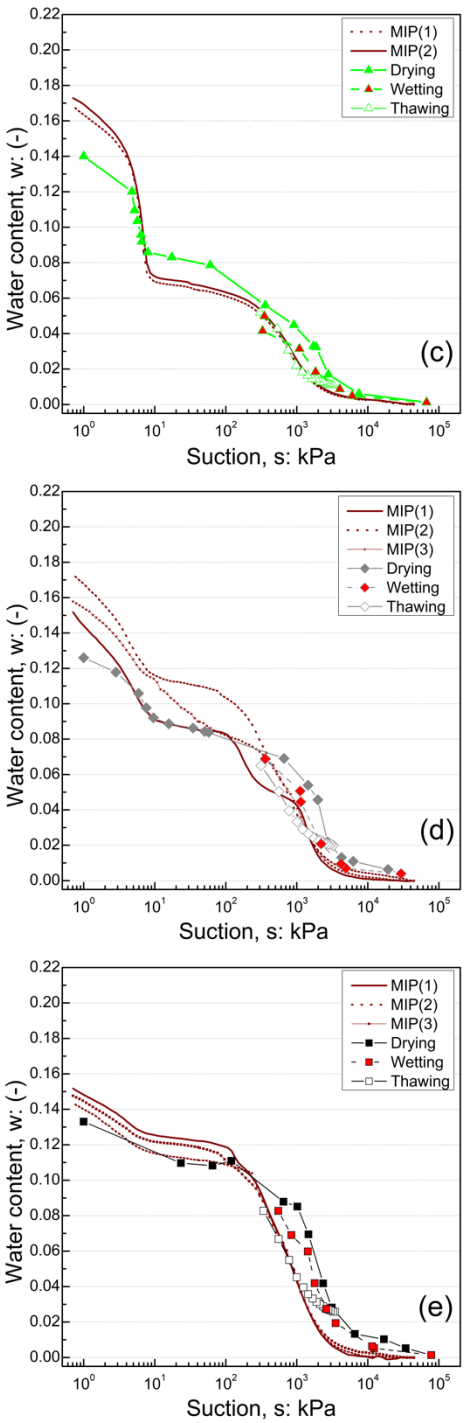

Fig. 8. SWRCs determined using the three methods for soils: (a) S0; (b) S5; (c) S10; (d) S15; (e) S20.

4 Conclusions

SWRCs of clayey sands (having clay content varying from 0 to 20%) were obtained by three methods. The results show that SWRCs estimated from mercury intrusion porosimetry and soil freezing characteristic curve are generally in agreement with the reference SWRC.

MIP tests can provide SWRC covering a wide range of suction (1 kPa to 40 MPa) which is appropriate for clayey sands. However, it underestimates water content at suction higher than 1000 kPa for sands with high clay content because it neglects the presence of adsorbed water on clay particles. In addition, results obtained by MIP test on sands with high clay content show significant discrepancy because of soil structure heterogeneity obtained by Proctor compaction.

Soil water characteristic curve can be used to estimate SWRC. However, this method is limited to a small suction range (500 kPa to 3 MPa in this study), which is not appropriate for clayey sands where a wider range is necessary to cover both macropores related to the arrangement of sand particles and micropores related to clay particles.

References

1. A.A. Abed, W.T. Sołowski, *A study on how to couple thermo-hydro-mechanical behaviour of unsaturated soils: Physical equations, numerical implementation and examples*, Comput Geotech **92**:132–155 (2017).
2. D. Sun, D. Sheng, L. Xiang, S.W. Sloan, *Elastoplastic prediction of hydro-mechanical behaviour of unsaturated soils under undrained conditions*, Comput Geotech **35**:845–852 (2008).
3. A. Zhou, D. Sheng, *An advanced hydro-mechanical constitutive model for unsaturated* soils *with different initial densities*, Comput Geotech **63**:46–66 (2015).
4. T. V. Duong, V.N. Trinh, Y.J. Cui, A.M. Tang, N. Calon, *Development of a Large-Scale Infiltration Column for Studying the Hydraulic Conductivity of Unsaturated Fouled Ballast*, Geotech Test J **36**:54–63 (2013).
5. D.G. Toll, S.D.N. Lourenço, J. Mendes, *Advances in suction measurements using high suction tensiometers*, Eng Geol **165**:29–37 (2013)
6. J.A. Blatz, Y.J. Cui, L. Oldecop, *Vapour Equilibrium and Osmotic Technique for Suction Control*. In: Laboratory and Field Testing of Unsaturated Soils, Springer Netherlands, Dordrecht, pp 49–61 (2008)
7. M.A. Rouf, S. Hamamoto, K. Kawamoto, T. Sakaki, T. Komatsu, P. Moldrup, *Unified measurement system with suction control for measuring hysteresis in soil-gas transport parameters*, Water Resour Res **48**:1–11 (2012)
8. T. Young, *III. An essay on the cohesion of fluids,* Philos Trans R Soc London 65–87 (1805)
9. P.S. Laplace, *Supplement to book 10 of Mecanique Celeste*, Crapelet, Courcier, Bachelier, Paris (1806)
10. W.B. Lindquist, A. Venkatarangan, J.R. Dunsmuir, T. Wong, *Pore and throat size distributions measured from synchrotron X-ray tomographic images of Fontainebleau sandstones*, J Geophys Res Solid Earth **105**:21509–21527 (2000)
11. M. Wang, G.N. Pande, L.W. Kong, Y.T. Feng *Comparison of Pore-Size Distribution of Soils Obtained by Different Methods*, Int J Geomech **17**:06016012 (2017)
12. P. Delage, M. Audiguier, Y.J. Cui, M. Deveughèle (1995), *Propriétés de rétention d'eau et microstructure de différents géomatériaux*, In: XIème Conférence Européenne de Mécanique des Sols et des Travaux de Fondations pp 43–48

13. A.C. Turturro, M.C. Caputo, H.H. Gerke, *Mercury intrusion porosimetry and centrifuge methods for extended-range retention curves of soil and porous rock samples*, Vadose Zo J **21**:1–11 (2022)
14. J.A. Muñoz-Castelblanco, J.M. Pereira, P. Delage, Y.J. Cui, *The water retention properties of a natural unsaturated loess from northern France*, Géotechnique **62**:95–106 (2012)
15. E. Romero, A. Gens, A. Lloret, *Water permeability, water retention and microstructure of unsaturated compacted Boom clay*, Eng Geol **54**:117–127 (1999)
16. N.E. Edlefsen, A.B.C Anderson *Thermodynamics of soil moisture*. Hilgardia **15**:31–298 (1943)
17. M. Bittelli, M. Flury, G.S. Campbell, *A thermodielectric analyzer to measure the freezing and moisture characteristic of porous media*, Water Resour Res **39** (2003)
18. K. Yoshikawa, P.P. Overduin, *Comparing unfrozen water content measurements of frozen soil using recently developed commercial sensors*, Cold Reg Sci Technol **42**:250–256 (2005)
19. J. Ren, S.K. Vanapalli, *Comparison of Soil-Freezing and Soil-Water Characteristic Curves of Two Canadian Soils*, Vadose Zo J **18**:1–14 (2019)
20. S.F. Santoyo, T. Baser, *A review of the existing data on soil-freezing experiments and assessment of soil-freezing curves derived from soil–water retention curves*, J Cold Reg Eng **36**:1–12 (2022)
21. K.V.Bicalho, F.V. Gonçalves, L.S. Favero *Evaluation of the Soil-Water Retention Curves of Different Unsaturated Silt-Sand Soil Mixtures*, In: PanAm Unsaturated Soils 2017 pp 95–103 (2017)
22. Y. Su, Y.J. Cui, J.C. Dupla, J. Canou, *Soil-water retention behaviour of fine/coarse soil mixture with varying coarse grain contents and fine soil dry densities*, Can Geotech J **59**:291–299 (2022).
23. S.K. Vanapalli, D.G. Fredlund, D.E. Pufahl, *The influence of soil structure and stress history on the soil–water characteristics of a compacted till*, Géotechnique **49**:143–159 (1999)
24. J.M. Baetens, K. Verbist, W.M. Cornelis, D. Gabriels, G. Soto, *On the influence of coarse fragments on soil water retention*, Water Resour Res 45 (2009)
25. C.P.K. Gallage, T. Uchimura, *Effects of Dry Density and Grain Size Distribution on Soil-Water Characteristic Curves of Sandy Soils*, Soils Found **50**:161–172 (2010)
26. C.H. Benson, I. Chiang, T. Chalermyanont, A. Sawangsuriya, *Estimating van Genuchten Parameters α and n for Clean Sands from Particle Size Distribution Data*, In: From Soil Behavior Fundamentals to Innovations in Geotechnical Engineering: Honoring Roy E. Olson, American Society of Civil Engineers pp 410–427 (2014)
27. A.S.S. Raghuram, B.M. Basha, A.A.B. Moghal, *Effect of Fines Content on the Hysteretic Behavior of Water-Retention Characteristic Curves of Reconstituted Soils*, J Mater Civ Eng **32**:04020057 (2020)
28. Q. Zhang, Z. Cao, C. Gu, Y. Cai, *Prediction of Soil–Water Retention Curves of Road Base Aggregate with Various Clay Fine Contents*, Appl Sci **12**:3624 (2022)
29. K. Boussaid, *Sols intermédiaires pour la modélisation physique : application aux fondations superficielles*, École Centrale de Nantes et Université de Nantes (2005)
30. A. Tarantino, D. Gallipoli, C.E. Augarde, V. D. Gennaro, R. Gomez, L. Laloui, C. Mancuso, G. E. Mountassir, J.J. Munoz, J.M. Pereira, H. Peron, G. Pisoni, E. Romero, A. Raveendiraraj, J.C. Rojas, D.G. Toll, S. Tombolato, S. Wheeler, *Benchmark of experimental techniques for measuring and controlling suction*, Géotechnique **61**:303–312 (2011)
31. V.T. Nguyen, H. Heindl, J.M. Pereira, A.M. Tang, J.D. Frost, *Water retention and thermal conductivity of a natural unsaturated loess*, Géotechnique Lett **7**:286–291 (2017)
32. Y. Wang, Y.J. Cui, A.M. Tang, N. Benahmed, W.J. Sun, *Shrinkage behaviour of a compacted lime-treated clay*, Geotech Lett **10**:174–178 (2020)
33. P. Delage, F.M. Pellerin, *Influence de la lyophilisation sur la structure d'une argile sensible du Québec*, Clay Miner **19**:151–160 (1984)
34. C. Doussan, S. Ruy, *Prediction of unsaturated soil hydraulic conductivity with electrical conductivity*, Water Resour Res **45**:1–12 (2009).
35. K. Yin, A.L. Fauchille, E.D. Filippo, K. Othmani, S. Branchu, G. Sciarra, P. Kotronis, *The Influence of Mixing Orders on the Microstructure of Artificially Prepared Sand-Clay Mixtures*, Adv Mater Sci Eng (2021)